Broadband Dielectric Investigation of Amorphous and Semicrystalline L-Lactide/*meso*-Lactide Copolymers

Mantana Kanchanasopa and James Runt*

Department of Materials Science & Engineering and Materials Research Institute, The Pennsylvania State University, University Park, Pennsylvania 16802

Received October 22, 2003; Revised Manuscript Received November 29, 2003

ABSTRACT: The dynamics of crystalline and amorphous samples of poly(L-lactide) and three L-lactide/*meso*-lactide random copolymers were investigated in the frequency domain using broadband dielectric spectroscopy (DRS). Two relaxations, the segmental (α) and subglass (β) processes, were observed in the temperature range between −100 and 105 °C. Modification of the characteristics of the α process, i.e., the relaxation strength ($\Delta\epsilon$), mean relaxation time (τ_m), and shape parameters, as a function of crystal content was investigated on "fully crystallized" samples as well as in real-time crystallization experiments. As expected, the strength of the α relaxation was smaller and its distribution broader for materials with higher degrees of crystallinity. The relaxation strength of the α process of the amorphous samples increased with temperature, while that of the crystalline materials changed very little or in the opposite direction with temperature. This behavior can be explained by the existence of a rigid amorphous component. Changes in τ_m and T_0 (the Vogel temperature) for the copolymers crystallized at various T_c are influenced by crystalline microstructure as well as by crystalline content. A relaxation is also observed in higher temperature (125−155 °C) experiments on amorphous and crystalline materials. The evidence at hand suggests that these processes are associated with the normal mode and α_c process, respectively.

Introduction

Polylactides are well-known as biocompatible and hydrodegradable polymers. Their intrinsic properties are of particular utility in biomedical applications (such as scaffolds for tissue engineering) as well as in larger volume applications. A number of studies have been conducted in an attempt to establish a fundamental understanding of this general class of polymers. For example, it was found that hydrolytic and enzymatic degradability of semicrystalline polylactides[1−3] is controlled by the degree of crystallinity and lamellar organization. In our previous work,[4−6] the influence of crystallization conditions and stereo-comonomer content on crystallinity, crystallization kinetics, and lamellar microstructure was investigated. Up to this point, we have paid only indirect attention to the characteristics of amorphous chain segments in these copolymers, including the critical role that the crystalline phase plays in influencing amorphous segment dynamics.

The main objective of the present study is to investigate the dynamics of fully amorphous and semicrystalline polylactides using broadband dielectric spectroscopy. The influence of the crystal phase on the chain dynamics of L-lactide/*meso*-lactide random copolymers will be discussed in the context of the relaxation strength ($\Delta\epsilon$), mean relaxation time (τ_{max}), and its distribution. Moreover, the presence of a so-called rigid amorphous phase is revealed from analysis of the fraction of mobile phase as a function of degree of crystallinity. Conclusions are arrived at based on results from a variety of semicrystalline samples (with crystallinity ranging from 30 to 70%) by varying *meso*-lactide content and crystallization conditions.

* To whom correspondence should be addressed: Tel 1-814-863-2749; Fax 1-814-865-2917; e-mail runt@matse.psu.edu.

Experimental Section

A. Materials and Sample Preparation. Poly(L-lactic acid) (PLLA) and L-lactide/*meso*-lactide stereocopolymers were synthesized at Cargill Dow Polymers. All polymers used in this study are rich in L-lactide (i.e., the *S* stereochemical isomer of lactic acid) and are crystallizable. Information on the characteristics of the four polymers is provided in Table 1. Previous NMR studies have shown that the copolymers are essentially random.[7]

Molecular weights of the polymers were determined by gel permeation chromatography, using tetrahydrofuran as the mobile phase and polystyrene molecular weight fractions as calibration materials. *R* stereochemical isomer content was determined by chiral liquid chromatography and reported in mole (or, equivalently, weight) percent.

For dielectric and DSC studies, films were prepared in a Carver laboratory hot press (model 2699). Films were sandwiched between two glass slides (covered with aluminum foil) and isothermally crystallized in a Mettler (model FP-82) hot stage. The surfaces of amorphous and crystalline films (with dimensions of ∼2.2 × 2.2 cm and ∼70−150 μm in thickness) were then gold-sputtered.

For isothermal crystallization, the samples were melted at 30 °C above their nominal melting point for 3 min in a hot stage and then transferred to a second hot stage preset at the crystallization temperature (T_c) and isothermally crystallized for t_c min. The crystallization conditions are the same as those used in our previous study and are described in ref 4. To obtain amorphous films, molten films were quenched into ice water for a short time (<1−2 min), wept dry right, and then maintained in a desiccator overnight before starting dielectric experiments. X-ray diffraction was utilized to ensure that all quenched films were noncrystalline.

B. Differential Scanning Calorimetry (DSC). Degrees of crystallinity were determined using a Perkin-Elmer DSC 7. Calibration was performed using indium as a standard. Approximately 3−5 mg of a particular sample was placed in an aluminum pan and scanned from 30 to 200 °C at a heating rate of 10 °C/min. The degree of crystallinity (X_c) was calculated by dividing the measured heat of fusion (ΔH_f) by 100 J/g, which is an estimate of ΔH_f^o for completely crystalline PLLA.[4]

10.1021/ma035597s CCC: $27.50
Published on Web 01/16/2004

Table 1. Characteristics of PLLA and L/*meso*-Lactide Copolymers

material	*R* (%)	M_n	M_w
PLLA	0.4	54 900	110 400
3% *meso*-lactide copolymer	2.1	54 900	109 700
6% *meso*-lactide	3.4	52 500	104 900
12% *meso*-lactide	6.6	57 600	113 500

C. Dielectric Measurements. Dielectric studies were carried out using a Novocontrol GmbH Concept 40 broadband dielectric spectrometer (DRS). Frequency sweeps from 6 MHz to 0.01 Hz were conducted isothermally. Temperature was controlled by a Novocontrol Quatro Cryosystem. While data collection was accomplished continuously from 105 (or 90) to −100 °C for the crystalline samples, it was separated into two scans for amorphous samples: dielectric spectra were first recorded from 40 to 74 °C to avoid the influence of crystallization at higher temperatures above T_g. Experiments at lower temperatures were then performed from 40 to −100 °C. Experiments up to higher temperatures (i.e., up to 155 °C) were conducted using the samples from the above experiments.

In a separate series of experiments, relaxation spectra for initially amorphous samples were collected during crystallization at 80 °C (from 6 MHz to 10 Hz) at ∼100 s intervals.

Analysis of Dielectric Spectra. Dielectric loss spectra in the temperature range of the glass transition were fitted with the Havriliak−Negami (HN) function:[8]

$$\epsilon^*(\omega) = \epsilon'(\omega) - i\epsilon''(\omega) \quad (1)$$

$$= \epsilon_\infty - i\sigma_0/(\epsilon_0\omega)^s + \Delta\epsilon/[1 + (\tau_m\omega)^a]^b \quad (2)$$

$\Delta\epsilon$ is the relaxation strength (i.e., equal to the interval between the relaxed and unrelaxed dielectric constants, i.e., $\epsilon_\infty - \epsilon_0$). The second term in eq 2 represents the contribution from dc conduction to the dielectric loss, where σ_0 is the dc conductivity constant in units of S/cm. The distribution of relaxation times (τ) is described by the central relaxation time (τ_m), a broadening parameter (a), and a parameter characterizing the skewness of the distribution (b). It is well-known that the segmental (α process) relaxation time distributions for crystalline and amorphous polymers are symmetric and asymmetric, respectively.[9] Consequently, the parameter b was fixed at 1 for fitting of the segmental process of the crystalline samples. In all preliminary fittings of the α process of amorphous samples, the parameter b was always found to be near 0.5. Therefore, it was fixed at 0.5 for all subsequent curve fitting.

Results and Discussion

Two relaxation processes, α and β, are observed in the dielectric relaxation spectra of amorphous and crystallized samples in the temperature range between −100 and 105 °C. Figure 1 presents isochronal plots of dielectric constant (ϵ') and loss (ϵ'') of PLLA crystallized at 141 °C. The broad local β process occurs at much lower temperatures compared to the relatively strong α segmental relaxation. The β-relaxation is believed to originate from local twisting motions of main chains.[10]

A. Subglass Process. Figure 2a presents peak positions (f_m) of the α and β processes of the amorphous PLLA and copolymers as a function of temperature. These data follow the Vogel−Fulcher−Tammann (VFT) and Arrhenius forms, respectively. Although not shown in Figure 2, the presence of the crystalline phase has no effect on the average relaxation time of the β process. Activation energies for the noncorrelated ester motion were determined to be in the range of 8−11 kcal/mol for all samples. These values compare very well with those reported for aliphatic polyesters in the literature (9−13 kcal/mol).[10−12]

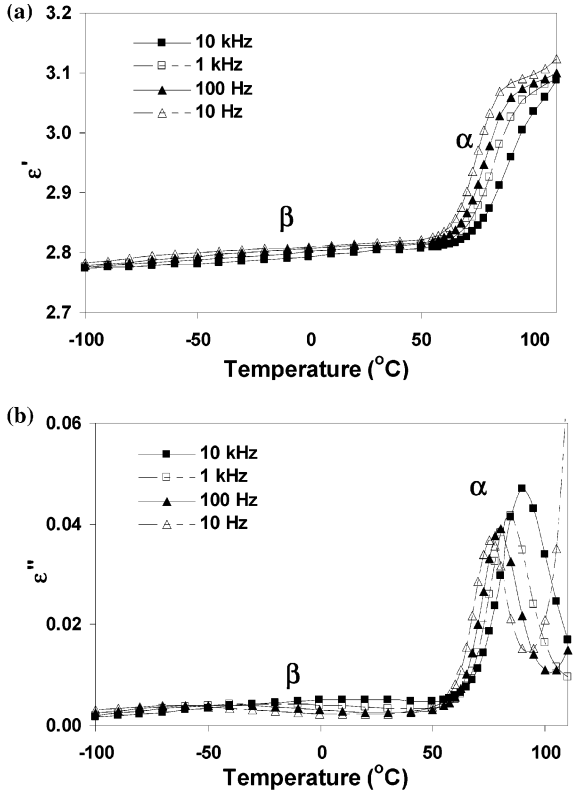

Figure 1. Isochronal plots of (a) dielectric constant and (b) dielectric loss of PLLA crystallized at 141 °C in frequency range from 10 Hz to 10 kHz.

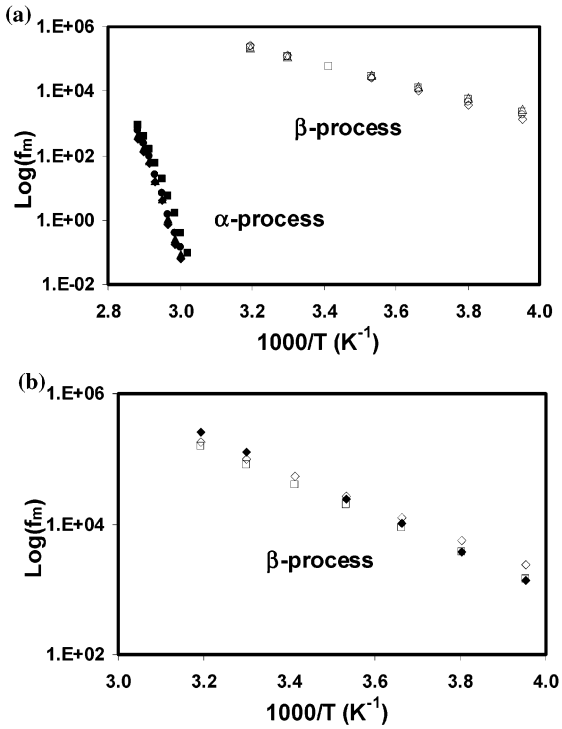

Figure 2. log f_m vs $1/T$ of (a) the α process (closed symbols) and β process (open symbols) of amorphous PLLA (◆) and 3% *meso*-lactide (▲), 6% *meso*-lactide (●), and 12% *meso*-lactide copolymers (■). (b) The β-process of amorphous PLLA (◆), PLLA crystallized at 90 °C (◇), and the crystallized 12% *meso*-lactide copolymer crystallized at 105 °C (□).

B. Segmental Relaxation. B.1. Crystallization from the Glassy State. To illustrate general trends in the segmental relaxation upon crystallization, we first

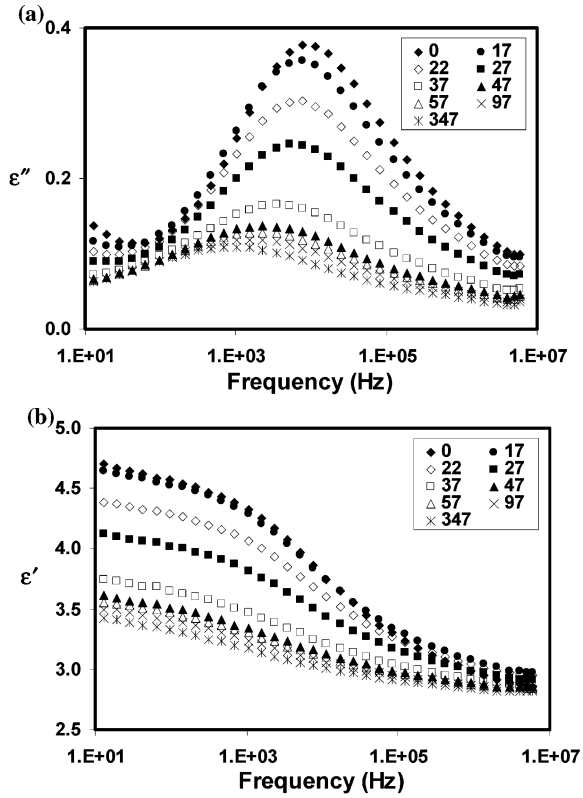

Figure 3. (a) Dielectric loss and (b) dielectric constant spectra during isothermal crystallization of the 3% *meso*-lactide copolymer at 80 °C as a function of t_c.

present the findings from a real-time crystallization experiment from the glassy state of an amorphous 3% *meso*-lactide copolymer at 80 °C. The results of similar experiments on the other (co)polymers under investigation are very similar and are not shown for brevity. Loss spectra (Figures 3a) exhibit significant changes in breadth and relaxation strength when t_c exceeds 17 min. The absence of changes at $t_c < 17$ min is not associated with an induction time, as crystallization is very rapid under these conditions, beginning within a few minutes of the sample reaching T_c. The fraction of mobile amorphous segments participating in the α process can be estimated from the ratio of the relaxation strength $(\epsilon'_\infty - \epsilon'_0)$ at t_c to that at $t_c = 0$ min (Figure 3b). The portion of mobile relaxing segments consumed at the point at which f_m begins to change significantly is ∼35% for this sample (i.e., at $t_c \sim 27$ min). Similar observations have been reported in real-time dielectric crystallization studies of poly(ethylene terephthalate) (PET),[13] poly(ether ether ketone),[14] and hydroxybutyrate−hydroxyvalerate copolymers.[12] There is no clear indication of two separate segmental processes in the loss spectra in Figure 3a, as has been observed during crystallization of PET.[15,16]

Up to $t_c = 17$ min, a large fraction of the relaxing segments are unconstrained, having mobility similar to that of segments of the completely amorphous sample. These include segments between growing spherulites as well as those between and within nascent lamellar stacks. However, the presence of the crystalline phase early in the crystallization process results in a broadening of the segmental relaxation process as the motion of a small portion of the relaxing segments becomes perturbed. The results of simultaneous wide- and small-angle X-ray scattering experiments on these same

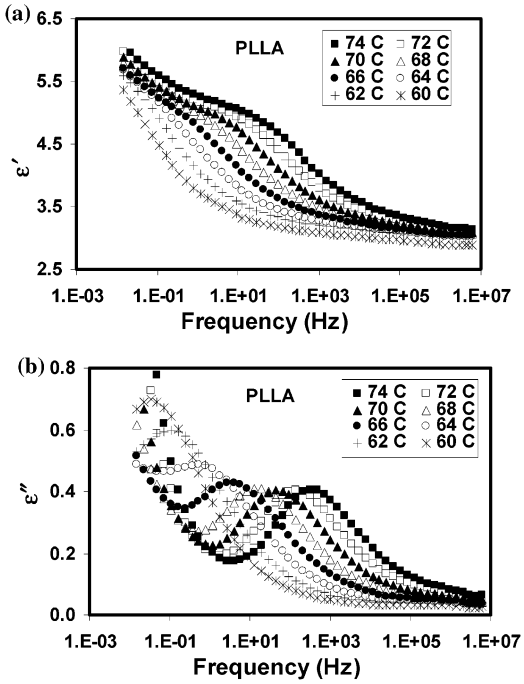

Figure 4. (a) Dielectric constant and (b) loss for amorphous PLLA as a function of frequency at the indicated temperatures.

polylactides during crystallization[17] suggest that crystallization of thinner lamellae or lamellar stacks occurs between dominant lamellae as crystallization proceeds and, together with the findings of "static" SAXS experiments,[4] supports a "finite stack" model for the final microstructure. Thus, either amorphous segments between dominant lamellae are "consumed" during crystallization, or their motion becomes quite constrained. In fact, a number of authors have argued that essentially all noncrystalline segments within relatively highly crystalline lamellar stacks are restricted from undergoing the usual segmental process.[14,18,19] As crystallization proceeds, the remaining mobile amorphous segments become constrained to varying degrees, giving rise to a net reduction in f_m and a broad relaxation resulting from a broad range of environments. Reduction in the relaxation strength with time arises from "consumption" of relaxing segments in the formation of lamellar crystals and in the formation of rigid amorphous segments, which will be discussed in more detail below.

Real-time DRS experiments of isothermal crystallization of the polylactides under investigation here can only be carried out within a limited temperature range due to relatively rapid crystallization from the glassy state. Consequently, investigation of the influence of crystallinity and microstructure on chain dynamics was primarily performed by comparing dielectric spectra of amorphous and "fully crystallized" samples.

B.2. Segmental Dynamics of Amorphous and Crystallized Samples. *B.2.1. Temperature-Dependent Dielectric Response.* The dielectric spectra of amorphous and semicrystalline PLLA are displayed in Figures 4 and 5, respectively. The presence of the crystalline phase alters the segmental relaxation in two significant ways. First, as discussed in the previous section, the relaxation strength declines dramatically, as anticipated from previous studies on crystalline polymers (e.g., ref 9). In addition, the temperature dependence of $\Delta\epsilon$ for the crystallized samples is opposite to that of the fully

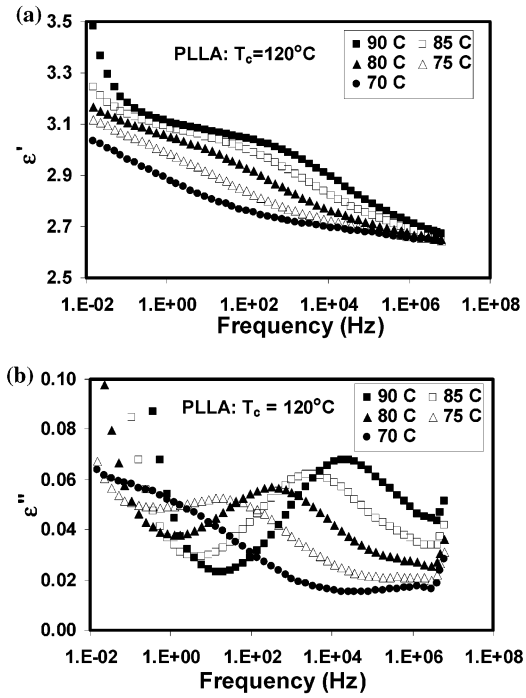

Figure 5. (a) Dielectric constant and (b) loss for PLLA crystallized at 120 °C as a function of frequency at the indicated temperatures.

amorphous ones, in which $\Delta\epsilon$ decreases with increasing temperature. Similar observations have been reported for other semicrystalline polymers.[20−22]

For the fully amorphous samples, the temperature-dependent behavior of $\Delta\epsilon$ is in good agreement with expectations from the Kirkwood−Onsager−Fröhlich equation: i.e., $\Delta\epsilon \propto N\mu^2 g/T$, where μ, N, and g are the dipole moment, number density of movable dipoles, and correlation factor, respectively.[23] If changes in g and N with temperature are negligible, this expression predicts that $\Delta\epsilon$ will decrease with increasing temperature (i.e., as a result of randomized dipoles with increasing temperature).

The idea of a rigid amorphous phase (RAP) has been introduced in order to explain the behavior of the crystalline materials. RAP segments are noncrystalline (unrelaxed at T_g) that have lower mobility compared to those of mobile amorphous segments (that relax near T_g).[24,25] RAP has been associated with segments in order−disorder interphases at crystal surfaces and, as noted above, with noncrystalline segments in interlamellar regions. It is likely that the mobility of these chain segments is enhanced at higher temperatures (above T_g), and $\Delta\epsilon$ would therefore be expected to increase with temperature.

Figure 6 presents the mean $\Delta\epsilon$ for the segmental process, based on the results of three specimens of each amorphous material. The error bars represent the standard deviation of each data point. As seen in Figure 4, only a portion of the PLLA segmental process is observed between 60 and 64 °C, and the uncertainty associated with curve fitting is therefore larger. From the results at higher temperatures, the strength of the segmental process is seen to depend on the chemical composition of the polymers. The influence of regioregularity on the chain conformations and flexibility of poly(lactic acid) polymers has been studied using Raman spectroscopy, light scattering,[26−28] and RIS Metropolis Monte Carlo calculations.[29] The characteristic ratios

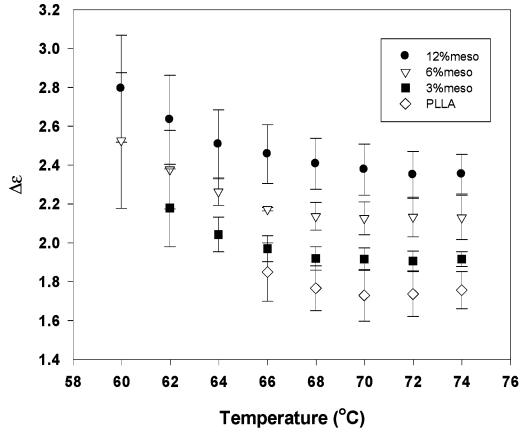

Figure 6. Relaxation strengths of amorphous samples of PLLA and the *meso*-lactide copolymers at the indicated temperatures.

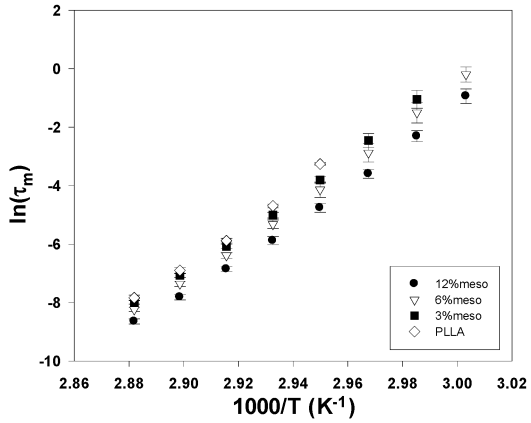

Figure 7. Mean relaxation times of amorphous PLLA and *meso*-lactide copolymers.

(C_∞) of lactic acid polymers have been found to decrease with increasing D-lactic acid content,[28] indicating that the copolymer chains are more flexible than those of the PLLA homopolymer. This conclusion is also supported by the present study: the somewhat higher relaxation strength (Figure 6) and lower τ_m (Figure 7) for the higher *meso*-lactide content copolymers.

B.2.2. Influence of the Crystalline Phase. The influence of the crystalline phase on the segmental τ_m is evident in Figure 8. DSC experiments reveal that, as expected, the crystallinities of the PLLA samples are higher than those of the copolymers, and the higher the *meso*-lactide content, the lower the crystallinity (Table 2). For PLLA, the presence of the relatively high crystallinity has an important effect on the average relaxation time of the α-process. The mean τ_m of the still mobile, yet perturbed, amorphous segments is much longer than that of the fully amorphous PLLA. Compared to PLLA, a smaller difference between τ_m of crystalline and amorphous samples is observed for copolymers with the higher *meso*-lactide contents (data not shown here). Eventually, there is no difference in τ_m between crystalline and amorphous samples for the 12% *meso*-lactide copolymer (Figure 8b). The latter results for these lowest crystallinity samples are similar to those reported recently for PLLA by Mijovic and Sy.[30] Therefore, our results suggest that crystalline content is the origin of the different observations for PLLA in the present study and those reported in ref 29. In addition, the data in ref 29 were acquired at 90−160 °C, compared with 75−90 °C

Table 2. Crystalline, Mobile, and RAP Fractions along with VFT Parameters and Fragilities for PLLA and the *meso*-Lactide Copolymers, Isothermally Crystallized at the Designated Temperatures

sample	material	T_c (°C)	$f_{crystal}$	f_{mobile}[a,b]	f_{RAP}[a]	T_0[c] (°C)	B[c]	T_{ref}[d] (°C)
amorphous	PLLA		0			21	1300	56
1		90	0.51	0.25	0.24	38	1060	67
2		120	0.60	0.27	0.13	33	1160	64
3		132	0.66	0.18	0.16	32	1140	63
4		141	0.68	0.18	0.14	34	1140	65
amorphous	3% meso		0			20	1300	55
5		120	0.48	0.31	0.21	23	1310	59
6		132	0.61	0.21	0.18	23	1290	58
7		135	0.58	0.21	0.21	22	1310	58
amorphous	6% meso		0			19	1320	55
8		120	0.47	0.35	0.18	21	1320	57
9		126	0.48	0.24	0.28	20	1320	56
10		132	0.55	0.24	0.21	19	1350	55
amorphous	12% meso		0			17	1340	54
11		105	0.34	0.33	0.33	16	1380	54
12		111	0.34	0.27	0.39	19	1320	54
13		117	0.38	0.22	0.40	16	1370	53

[a] Based on calculation at $T \sim T_0 + 50$ °C. [b] The fraction of mobile component determined from DRS was converted to mass fraction by multiplying by ρ_a/ρ_s, where ρ_a and ρ_s are the fully amorphous and sample densities, respectively. Densities of fully crystalline and amorphous PLLA have been reported to be 1.378 and 1.258 g/cm^3, respectively.[47] Sample densities were estimated from $[\rho_c \times f_{crystal}] + [\rho_a \times 1 - f_{crystal}]$. [c] Standard deviation of VFT parameters: within ~5% for B and ~1 °C for T_0. [d] Temperature at which $\tau_{max} = 100$ s.

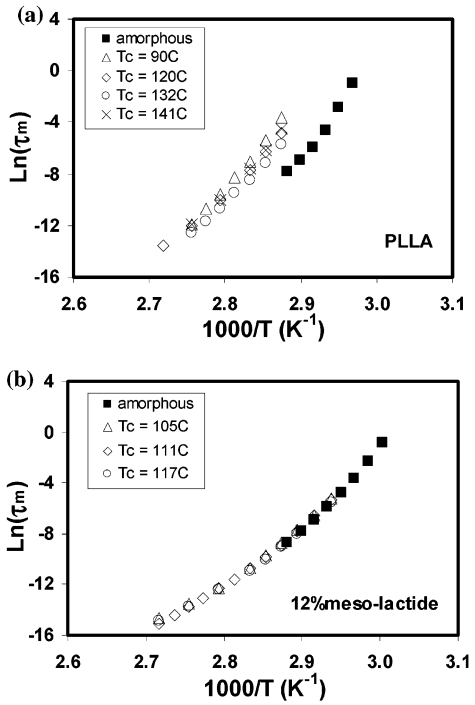

Figure 8. Comparison between the relaxation time of the amorphous and crystallized samples of (a) PLLA and (b) 12% *meso*-lactide copolymer.

in the present study: at higher temperatures, it is likely that constraints imposed on restricted amorphous segments would be relaxed.

A careful examination of Figure 8a leads to the conclusion that the segmental dynamics of crystallized PLLA is also determined by crystallization conditions. The somewhat longer τ_m for the sample crystallized at 90 °C implies that, on average, more significant constraints (e.g., arising from the relatively large fraction of amorphous segments residing in tie-chains between lamellae) are imposed on mobile amorphous segments in this sample compared with those crystallized at the higher temperatures. This is not due to crystalline content since the crystallinity of this sample is lower than the others. Other findings[31] also support the idea that the crystal microstructure developed at low T_c during very rapid crystallization is an important factor influencing segmental dynamics. At $T_c = 90$ °C, although the spherulite growth rate is below its maximum value (observed at $T_c \sim 126-129$ °C for PLLA[4]), the primary nucleation rate is quite high. In fact, crystallization on cooling from the melt is undoubtedly nonisothermal at this T_c due to very rapid crystallization. The crystal microstructure developed under these conditions is likely composed of "mobile" amorphous segments that are relatively constrained due to the rapid solidification. Copolymers with 3 and 6% *meso*-lactide demonstrate similar behavior (not shown).

The experimental τ_m were fit with the VFT equation:[32]

$$\tau_m = \tau_0 \exp(B/(T - T_0)) \quad (3)$$

where τ_0 is a prefactor correlated to the time scale at which the molecules are attempting to overcome an energy barrier, B is related to the strength for glass-forming, and T_0 is a temperature below T_g at which the segments become frozen. Taking τ_0 to be 10^{-14} s,[33] B and T_0 were calculated for the amorphous and crystallized materials, and these are summarized in Table 2. The parameter B is related to the fragility, m, a measure of the rapidity with which a material changes its mean relaxation time in the vicinity of T_g:[34]

$$m = \frac{B}{T_{ref} \ln 10 \left(1 - \frac{T_0}{T_{ref}}\right)^2} \quad (4)$$

where T_{ref} is a reference temperature, defined here as the temperature at which $\tau_{max} = 100$ s, and normally takes on value close to T_g obtained from standard scanning measurements.[35] Within experimental uncertainity, the calculated fragilities for all amorphous and crystalline samples are the same ($m \sim 150$, defining T_{ref} as above). The invariance of m in the presence and with degree of crystallinity is in keeping with previous findings.[30,36]

Values for T_{ref} are summarized in Table 2 for the various materials under investigation in this study. There is no difference between T_{ref} of the amorphous PLLA and *meso*-lactide copolymers, consistent with our

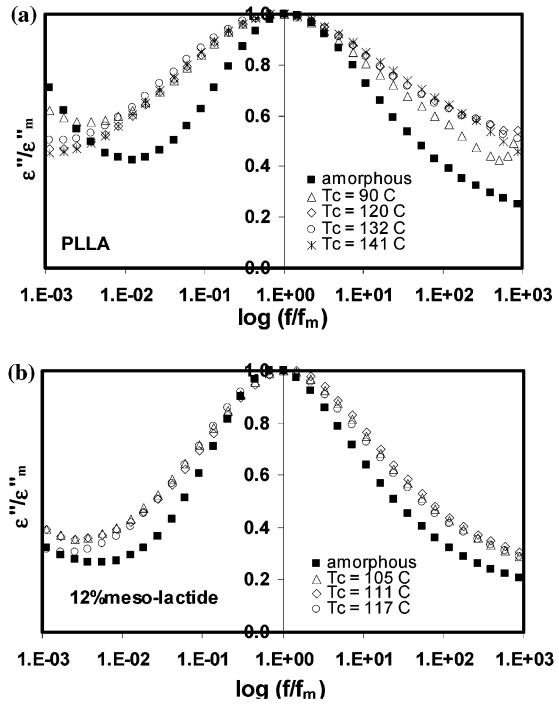

Figure 9. ϵ''/ϵ''_m vs $\log(f/f_m)$ for (a) amorphous and crystallized PLLA and (b) amorphous and crystallized 12% *meso*-lactide copolymer.

previous measurement of T_gs of these materials by DSC.[4] However, T_{ref} increases by about 10 °C for crystallized PLLA, not an uncommon observed for crystallizable polymers, but changes very little (if at all) for the lower crystallinity copolymers. In general, a slightly higher T_g has been observed in other studies for samples crystallized at lower T_c (both cold and melt-crystallization) as well as from nonisothermal crystallization at higher cooling rates (e.g., refs 21 and 37), and it does appear that T_{ref} is slightly higher for the PLLA crystallized at 90 °C.

Normalized loss plots [ϵ''/ϵ''_m vs $\log(f/f_m)$] are depicted in parts a and b of Figure 9 for the amorphous and crystallized samples of PLLA and the 12% *meso*-lactide copolymer, respectively. These figures present dielectric loss spectra at comparable temperatures, i.e., at $T = T_0 + 50$ °C and $T_0 + 55$ °C for PLLA and 12% *meso*-lactide copolymer, respectively. Compared with the amorphous samples, it is apparent that the relaxations are broader and more symmetrical when crystallinity is present. The fitted broadening parameters (a) are plotted in Figure 10 (for samples crystallized at or near 120 °C) as a function of temperature, demonstrating the influence of crystallinity. Smaller values of a (i.e., broader segmental processes) are observed for crystalline PLLA, in contrast to the lower crystallinity copolymers.

B.2.3. The Rigid Amorphous Phase. Since the strength of the α relaxation is characteristic of the mobile phase, the fraction of mobile amorphous segments (f_{mobile}) in the crystallized samples that relax at a given temperature can be written as[21]

$$f_{mobile}(T) = \Delta\epsilon_{sc}(T)/\Delta\epsilon_{am}(T) \qquad (5)$$

where $\Delta\epsilon_{sc}$ and $\Delta\epsilon_{am}$ are the relaxation strength of the crystallized and fully amorphous samples, respectively. The rigid segment fraction (f_{rigid}) is therefore simply $f_{rigid}(T) = 1 - f_{mobile}(T)$. To obtain f_{mobile}, values of $\Delta\epsilon_{sc}$ and

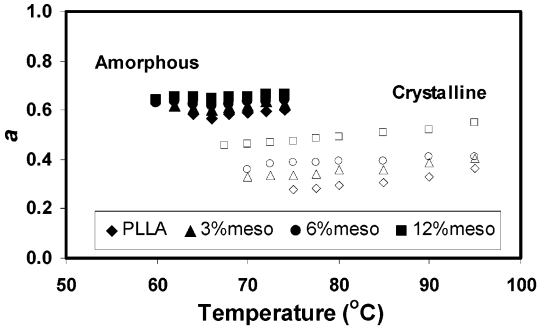

Figure 10. HN broadening parameter, a, of amorphous (closed symbols) and PLLA, 3% and 6% *meso*-lactide copolymers crystallized at T_c = 120 °C, and 12% *meso*-lactide copolymer crystallized at T_c = 117 °C (open symbols used for crystallized samples): ◆, PLLA; ▲, 3% *meso*-lactide; ●, 6% *meso*-lactide; ■, 12% *meso*-lactide.

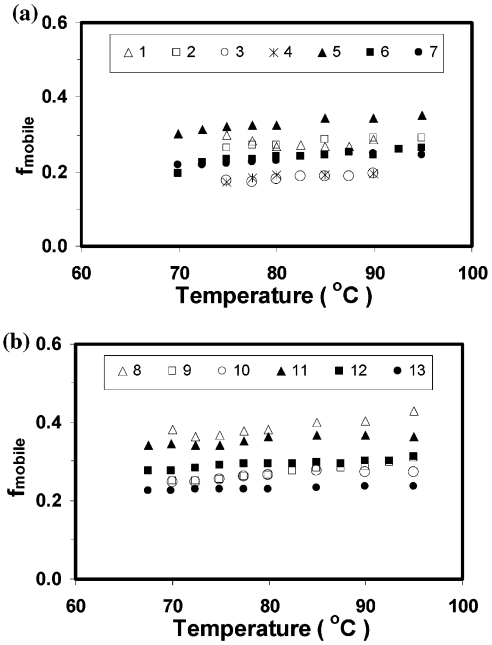

Figure 11. Fraction of mobile phase as a function of temperature. Numbers in the figure legend correspond to the sample number listed in Table 2.

$\Delta\epsilon_{am}$ at the same temperature are required. This is not feasible in the present case since crystallization occurs at temperatures above 74 °C for the amorphous samples. Since $\Delta\epsilon_{am}$ was found (Figure 6) to be constant above 68 °C for the different polymers, $\Delta\epsilon_{am}$ at temperatures above 74 °C was assumed to take on these "limiting" values. Finally, since the dielectric relaxation strength is proportional to the number of dipoles per unit volume of a sample, to compare f_{mobile} with $f_{crystal}$ determined from DSC or WAXD (and to calculate f_{RAP} consistently), $f_{mobile}(T)$ should be converted to mass fractions. Details of this conversion are reported under Table 2. The changes in f_{mobile} are relatively small, i.e., on the order of ~0.01.

Values of f_{mobile} (mass fraction) as a function of temperature for the crystallized samples are displayed in Figure 11. (The samples are identified by a number corresponding to Table 2.) f_{mobile} appears to increase slightly with temperature for all but one sample (sample 1), consistent with the idea of progressive loss of constraint for rigid amorphous segments. However, caution must be exercised here since the uncertainty

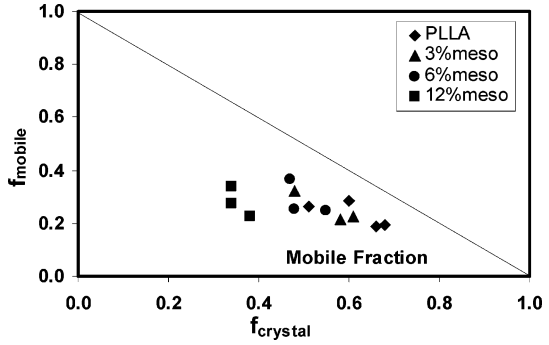

Figure 12. Mobile segment fraction vs crystalline fraction for all samples investigated.

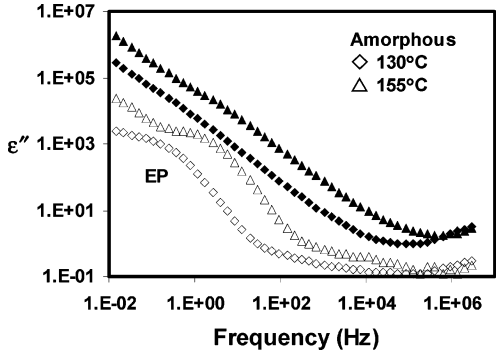

Figure 13. Plot of log ϵ'' (closed symbols) and log ϵ''_{der} (open symbols) at 130 (◇) and 155 °C (△) for the amorphous 12% *meso*-copolymer. Data of ϵ'' were multiplied by 10 to offset its plots from the ϵ''_{der} plots.

in f_{mobile} is estimated to be on the order of several percent.

The lowest temperature at which the α process can be resolved without significant uncertainty due to overlap from dc conduction is in the range of ∼75−67.5 °C (from PLLA to the copolymers). Therefore, comparison of f_{mobile} and f_{RAP} between the crystalline samples was made at T_0 + 50 °C (Table 2). The relationship between f_{mobile} and $f_{crystal}$ is presented in Figure 12. The data for PLLA and the copolymers clearly deviate from the prediction for a simple two-phase model (solid line). As noted earlier, the crystallinities in Table 2 and Figure 12 were determined using DSC and $\Delta H_f^o = 100$ J/g.[4] Since other values for ΔH_f^o for PLLA have appeared in the literature,[31,38,39] we confirmed the crystallinities using wide-angle X-ray diffraction (WAXD) measurements. This was accomplished by dividing the area under the crystalline *x*-reflections in the 2θ range from 5° to 30° by the total area (crystalline reflections + amorphous halo). In fact, the WAXD values and those determined from DSC using 100 J/g for ΔH_f^o were found to be in very good agreement.

For semiflexible poly(ether ketone ketone)[37] and poly(phenylene sulfide)[40] copolymers, the difference between the T_gs of amorphous and crystalline samples is lower for copolymers with higher comonomer content—as observed here. This was correlated with lower rigid amorphous phase content, which is reduced as more flexible meta-linkages are incorporated into the para-connected homopolymers. In contrast, however, the impact of *meso*-lactide comonomer on f_{RAP} is not observed for the polylactide copolymers. This is good evidence that the effectiveness of the crystal phase in hindering the segmental relaxation does not simply depend on the crystallinity and RAP content, but also on an effective size of the noncrystalline phase modified during the crystallization process.[41,42]

C. Higher Temperature Relaxations. In addition to the primary focus on the segmental process of PLLA and the copolymers, we also investigated the dielectric relaxation behavior at higher temperatures. Since losses due to dc conduction are very strong in this higher temperature range, we employ an alternative representation of the experimental loss factor data. The first derivative of the real part of the dielectric constant (ϵ') has been shown to be a good approximation of the Kramers−Kronig transform of ϵ' to ϵ'' and to provide an "ohmic conduction-free" dielectric loss, ϵ''_{der}:[43]

$$\epsilon''_{der} = -\frac{\pi}{2}\frac{\partial \epsilon'(f)}{\partial \ln f} \qquad (6)$$

In a series of model calculations, ϵ''_{der} and ϵ'' have been demonstrated to exhibit the same peak frequencies, and as long as the relaxations are relatively broad (as they are in our case), the relaxation strength of a derivative spectrum is a very good approximation to that of ϵ''.[44]

To avoid crystallization during the course of the DRS experiment, spectra were acquired for the amorphous 12% *meso*-lactide copolymer in the temperature range from 130 to 155 °C (see Figure 13). The log ϵ'' and log ϵ''_{der} spectra at two temperatures are presented in Figure 13. Many characteristics of the high loss at lower frequency are what are expected from electrode polarization:[44] very high dielectric constant (within the range of 10^2-10^6, not shown) and scaling of the slopes of the experimental and derivative loss spectra at higher frequencies with ω^{-1} and ω^{-2}, respectively.

Careful examination of the ϵ''_{der} spectra (on both log and linear scales) suggests a small shoulder at higher frequencies (f_m ∼ ca. 10^4 Hz) of lower strength The relaxation time associated with global chain dynamics (α_n) is well-known to depend strongly on molecular weight, i.e., $\tau_{normal} \propto M_n^x$ where $x \sim 3.1-3.5$.[11,45] On the basis of the VFT parameters reported in ref 11, α_n is estimated to be near $f_m \sim 20-100$ Hz, in the temperature range 125−155 °C, i.e., within ∼2 decades of the observed process. Therefore, given the approximate nature of the estimate, the similarity of the relaxation strength with that reported in ref 11, and that the sample is in the melt at these temperatures, this process is assigned to the normal mode of the 12% *meso*-lactide copolymer chains.

DRS spectra (log ϵ''_{der}) at three temperatures between 125 and 145 °C for PLLA crystallized at 90 °C are shown in Figure 14a. A process is clearly observed in the range of ca. 1−10 Hz. This could originate from an α_c process, arising from local motion in the crystalline phase,[9] Maxwell−Wagner−Sillars (MWS) interfacial polarization,[46] or possibly electrode polarization. It is difficult to distinguish between these assignments, although the peak position is comparable to that reported for the α_c relaxation in mechanical loss spectra of PLLA.[47,48] A process at a similar frequency is observed in the 125 and 135 °C spectra of the 12% *meso*-lactide copolymer crystallized at 105 °C (Figure 14b). In the 145 °C DRS spectrum, the loss at low frequencies rises appreciably. Again, given the very high dielectric constant (>10^2, not shown) and the scaling of the "high-frequency" slopes of the log ϵ'' and log ϵ''_{der} representations in this frequency range, this is undoubtedly associated with electrode polarization.[44] It is important to note that 145

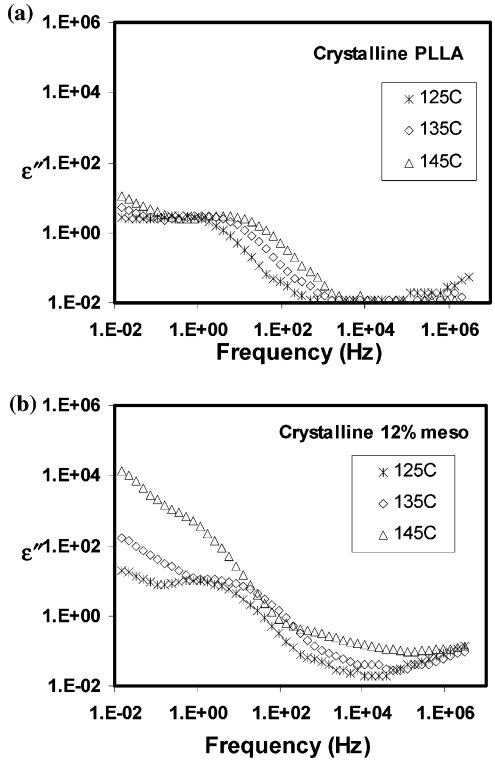

Figure 14. Plots of ϵ''_{der} vs frequency at 125 (∗), 135 (◇), and 145 °C (△) for (a) crystalline PLLA (T_c = 90 °C) and (b) 12% *meso*-lactide copolymer (T_c = 105 °C).

°C > T_m of the 12% copolymer (∼140 °C), hence the similarity to the spectra in Figure 13. Note the appreciable intensity near 10^4 Hz in the 145 °C spectrum, similar to the spectra of the amorphous 12% copolymer in Figure 13. This result supports the assignment of the relaxation in this region to the normal mode (α_n).

Summary

In this paper we summarize our DRS investigation of the dynamics of amorphous segments in fully amorphous and semicrystalline PLLA and three L-lactide/*meso*-lactide copolymers. The difference in temperature-dependent behavior of the relaxation strength of the α process for amorphous and crystalline samples is consistent with the presence of a rigid amorphous component. Higher degrees of crystallinity generally result in lower $\Delta\epsilon$, longer τ_m, and broader the relaxation time distributions. Although it initially appears that the crystallinity is the overriding factor controlling the characteristics of the α-process, a detailed analysis reveals that the crystalline microstructure also play an important role.

A process is observed at higher temperatures (125−155 °C) for the amorphous 12% *meso*-lactide copolymer at 10^2−10^4 Hz. Evidence at hand suggests that this is associated with the global chain relaxation (α_n). The very pronounced process observed at lower frequencies (10^{-1}−10^2 Hz) in these samples undoubtedly arises from electrode polarization. The origin of the process in this temperature range in crystallite samples remains uncertain, although it occurs near the in the temperature range at which the α_c process has been observed in mechanical experiments.

Acknowledgment. The authors express their appreciation to the donors of the ACS Petroleum Research Fund and the National Science Foundation (DMR-0211056) for their support of this work. We also thank Mr. Eric Hall at Cargill Dow for providing the polymers used in this study and colleagues at Cargill Dow for determining molecular weights and performing chiral chromatography analysis.

References and Notes

(1) Makino, K.; Arakawa, M.; Kondo, T. *Chem. Pharm. Bull.* **1985**, *33*, 1195.
(2) Reeve, M.; McCarthy, S.; Downey, M.; Gross, R. *Macromolecules* **1994**, *27*, 825.
(3) MacDonald, R.; McCarthy, S.; Gross, R. *Macromolecules* **1996**, *29*, 7356.
(4) Huang, J.; Lisowski, M. S.; Runt, J.; Hall, E. S.; Kean, R. T.; Buehler, N.; Lin, J. S. *Macromolecules* **1998**, *31*, 2593.
(5) Kanchanasopa, M.; Manias, E.; Runt, J. *Biomacromolecules* **2003**, *4*, 1203.
(6) Baratian, S.; Hall, E. S.; Lin, J. S.; Xu, R.; Runt, J. *Macromolecules* **2001**, *34*, 4857.
(7) Thakur, K. A. M.; Kean, R. T.; Hall, E. S.; Kolstad, J. J.; Lindgren, T. A.; Doscotch, M. A.; Siepmann, J. I.; Munson, E. J. *Macromolecules* **1997**, *30*, 2422.
(8) Havriliak, S.; Negami, S. *J. Polym. Sci., Polym. Symp.* **1966**, *14*, 99.
(9) Boyd, R. H. *Polymer* **1985**, *26*, 323. Boyd, R. H. *Polymer* **1985**, *26*, 1123.
(10) Starkweather, H. W.; Avakian, P. *Macromolecules* **1993**, *26*, 5084.
(11) Mierzwa, M.; Floudas, G.; Dorgan, J.; Knauss, D.; Wegner, J. *J. Non-Cryst. Solids* **2002**, *307*−*310*, 296.
(12) Nogales, A.; Ezquerra, T. A.; Garcia, J. M.; Balta-Calleja, F. J. *J. Polym. Sci., Polym. Phys.* **1999**, *37*, 37.
(13) Ezquerra, T. A.; Balta-Calleja, F. J.; Zachmann, H. G. *Polymer* **1994**, *35*, 2600.
(14) Nogales, A.; Ezquerra, T. A.; Denchev, Z.; Sics, I.; Balta-Calleja, F. J.; Hsiao, B. S. *J. Chem. Phys.* **2001**, *115*, 3804.
(15) Alves, N. M.; Mana, J. F.; Balaguer, E.; Mesequer Duenas, J. M.; Gomez Ribelles, J. L *Polymer* **2002**, *43*, 4111.
(16) Ezquerra, T. A. Unpublished results.
(17) Cho, J. D.; Baratian, S.; Kim, J.; Yeh, F.; Hsiao, B. S.; Runt, J. *Polymer* **2003**, *47*, 711.
(18) Lin, J.; Shenogin, S.; Nazaranko *Polymer* **2002**, *43*, 4733.
(19) Ivanov, D. A.; Pop, T.; Yoon, D. Y.; Jonas, A. M. *Macromolecules* **2002**, *53*, 9813.
(20) Schlosser, E.; Schonhals, A. *Colloid Polym. Sci.* **1989**, *267*, 963.
(21) Huo, P.; Cebe, P. *Macromolecules* **1992**, *25*, 902. Huo, P.; Cebe, P. *Polymer* **1992**, *30*, 239.
(22) Nogales, A.; Denchev, Z.; Sics, I.; Ezquerra, T. A. *Macromolecules* **2000**, *33*, 9367.
(23) McCrum, N. G.; Read, B. E.; Williams, G. *Anelastic and Dielectric Effects in Polymeric Solids*; Dover Publications: New York, 1991.
(24) Schick, C.; Wurm, A.; Mohammed, A. *Thermochim. Acta* **2003**, *396*, 119.
(25) Pak, J.; Pyda, M.; Wunderlich, B. *Macromolecules* **2003**, *36*, 495.
(26) Kang, S.; Hsu, S. L. *Macromolecules* **2001**, *34*, 4542.
(27) Yang, X.; Kang, S.; Hsu, S. L.; Stidham, H. D.; Smith, P. B.; Leugers, A. *Macromolecules* **2001**, *34*, 5037.
(28) Kang, S.; Zhang, G.; Aou, K.; Hsu, S. L.; Stidman, H.; Yang, X. *J. Chem. Phys.* **2003**, *118*, 3430.
(29) Blomqvist, J. *Polymer* **2001**, *42*, 3515.
(30) Mijovic, J.; Sy, J. W. *Macromolecules* **2002**, *35*, 6370.
(31) Iannace, S.; Nicolais, L. *J. Appl. Polym. Sci.* **1997**, *64*, 911.
(32) Ferry, J. D. *Viscoelastic Properties of Polymers*; Wiley: New York, 1980.
(33) Jin, X.; Zhang, S. H.; Runt, J. *Macromolecules* **2003**, *36*, 8033.
(34) Angell, C. A. *Science* **1995**, *267*, 1924.
(35) Angell, C. A. *J. Non-Cryst Solids* **1991**, *131*−*133*, 13.
(36) Ngai, K. L.; Roland, C. M. *Macromolecules* **1993**, *26*, 6824.
(37) Kalika, D. S.; Krishnaswamy, R. K. *Macromolecules* **1993**, *26*, 4252. Krishnaswamy, R. K.; Kalika, D. S. *Polymer* **1996**, *37*, 1915.
(38) Fischer, E. W.; Sterzel.; Wegner, H. J. *Kolloid Z. Z. Polym.* **1973**, *251*, 980.
(39) Cohn, D.; Younes, H.; Marom, G. *Polymer* **1987**, *28*, 2018.
(40) Kalika, D. S.; Wu, S. S. *J. Macromol. Sci., Phys.* **1996**, *B35*, 179.
(41) Schick, C.; Nedbal, J. *Prog. Colloid Polym. Sci.* **1988**, *78*, 9.

(42) Huo, P.; Cebe, P. *Colloid Polym. Sci.* **1992**, *270*, 840.
(43) Steeman, P. A. M.; van Turnhout, J. *Macromolecules* **1994**, *27*, 5421.
(44) Wübbenhorst, M.; van Turnhout, J. *J. Non-Cryst. Solids* **2002**, *305*, 40.
(45) Ren, J.; Urakama, O.; Adachi, K. *Macromolecules* **2003**, *36*, 210.
(46) Hayward, D.; Pethrick, R. A.; Siriwittayakorn, T. *Macromolecules* **1992**, *25*, 1480.
(47) Urayama, H.; Kanamori, T.; Kimura, Y. *Macromol. Mater. Eng.* **2001**, *286*, 705.
(48) Pluta, M.; Galeski, A. *J. Appl. Polym. Sci.* **2002**, *86*, 1386.

MA035597S